

Bundle Formation in Polyelectrolyte Brushes

J. U. Günther,¹ H. Ahrens,¹ S. Förster,² and C. A. Helm¹

¹*Institut für Physik, Universität Greifswald, Felix-Hausdorff-Str. 6, D-17487 Greifswald, Germany*

²*Institut für Physikalische Chemie, Universität Hamburg, Grindelallee 117, D-20146 Hamburg, Germany*

(Received 10 February 2006; revised manuscript received 19 September 2008; published 19 December 2008)

Bundle formation of the vertically oriented polyelectrolytes within polyelectrolyte brushes is studied with x-ray reflectivity and grazing-incidence diffraction as a function of grafting density and ion concentration. At 0.8 Molar monomer concentration and without added salt, a bundle consists of two chains and is 50 Å long. On the addition of up to 1M CsCl, the aggregation number increases up to 15 whereas the bundle length approaches a limiting value, 20 Å. We suggest that the bundle formation is determined by a balance between long-ranged electrostatic repulsion, whose range and amplitude is decreased on salt addition, and short-ranged attraction.

DOI: 10.1103/PhysRevLett.101.258303

PACS numbers: 82.35.Rs, 82.35.Lr

Linear polyions in solution repel each other and form strongly structured fluids. Thus, Bragg peaks are detected with scattering methods [1]. At high polyion concentrations c_p , their nearest neighbor distance d scales with the square root of c_p . To explain this relationship, de Gennes *et al.* [2] proposed a detailed model of flexible polyelectrolytes at low ionic strength and high polyion concentrations c_p . Different chains overlap each other, and several arrangements were discussed: (a) a lattice of rigid rods and (b) an isotropic phase of entangled and thus partially flexible chains. The latter case is assumed to be the most probable structure. Each chain consists of connected, randomly oriented segments. Within one segment, electrostatic effects dominate and induce an elongated segmental conformation (i.e., an increased persistence length), whereas between different segments, the interactions are completely screened. For this model, the average distance as derived from the Bragg peaks is $d = \sqrt{2} f c_p^{-1/2}$, where f depends on the lattice geometry (hexagonal, square, etc.) [3]. Therefore, an exponent of $-1/2$ does not necessarily indicate an ordered array of rigid rods, but may also originate from an isotropic network of entangled chains [1]. Experimentally, in the semidilute concentration regime, all experimental points obtained from various polyelectrolytes fall onto a common line, with the predicted power law dependence. However, the measured lattice distance in dilute solutions is larger than expected for aligned rods, a phenomenon yet unexplained.

Bundle formation would explain those scattering data. Stiff polyelectrolytes like DNA are found to spontaneously form oriented bundles under suitable electrostatic conditions [4,5]. Bundle size and length for more flexible polyions can be investigated with the vertically aligned and oriented chains of polyelectrolyte brushes, with a brush thickness between 30 and 50% of the contour length [6,7]. Polyelectrolyte brushes show two distinctly different regimes called “osmotic brush” and “salted brush,” respectively. In both phases, the ions compensating the polymer charges are incorporated into the brush [8–10]. In the

“osmotic brush” regime, the osmotic pressure of the counterions leads to strong stretching of the polyelectrolyte chains. An increase of grafting density increases the brush height slightly, due to the finite volume of monomers and ions [7]. However, the effect of added salt is considerable when the salt concentration in the bulk solution becomes comparable to or larger than the intrinsic ionic strength inside the brush (“salted brush”). Then, a power law dependence of the brush thickness on the molecular area and the bulk ion concentration is predicted and found. The polyelectrolyte brushes are prepared from monolayers at the air/water interface, a large self-annealing surface which is easily accessible to x-ray methods.

Materials.—The amphiphilic diblock copolymer consists of a fluid hydrophobic (PEE, polyethylene) and a polyelectrolyte block (PSS, polystyrenesulfonate), PEE₁₄₄PSS₁₃₆. Monolayers are prepared as described before [6]; the isotherms show hysteresis on compression/expansion cycles only at high salt concentrations ($c_s \geq 0.5M$).

Grazing-incidence diffraction measurements were performed at the liquid surface diffractometer at the beam line BW1 in HASYLAB [11–13]. With this technique, an x-ray beam strikes the surface at grazing-incidence angle α_i . If the electron density on the surface is laterally periodical, the evanescent wave is diffracted, and one observes Bragg peaks. A position sensitive detector measures the diffracted intensity at exit angle α_f and in-plane scattering angle θ . The interplanar spacing d is deduced from the maximum position of the Bragg peak Q_{xy}^{\max} according to the Bragg condition $d = 2\pi/Q_{xy}^{\max}$. If the scattering centers are aligned perpendicular to the surface, their vertical length L determines the intensity decay $I(Q_z) \propto (\frac{\sin(\frac{1}{2}LQ_z)}{Q_z})^2$, the so-called Bragg rod. If L approaches zero, the intensity of the Bragg rod is almost constant in Q_z direction. The experimental parameters are wavelength $\lambda = 1.303$ Å, critical angle $\alpha_c = 0.129^\circ$, incident angle $\alpha_i = 0.85\alpha_c$, and penetration depth $\Lambda = 85$ Å [12,13].

X-ray reflectivity.—The x-ray reflectivity of a PEE₁₄₄PSS₁₃₆ monolayer in the subphase is given as a function of wave vector transfer $Q_z = 4\pi/\lambda \sin\alpha$ with $\alpha = \alpha_i = \alpha_f$. The reflectivity R divided by the Fresnel reflectivity R_F expected for an infinitely sharp interface is given by [12,14] $\frac{R}{R_F} = \left| \frac{1}{\rho_{\text{sub}}} \int \frac{\partial \rho}{\partial z} \exp(iQ_z z) dz \right|^2$.

To derive the electron density profile $\rho(z)$ of PEE₁₄₄PSS₁₃₆, we use a slab model [6,7,12]. One slab describes the hydrophobic anchoring group. Below it, a thin and dense layer represents a PSS monolayer adsorbed to the hydrophobic PEE block. Three less dense and elongated slabs model the continuously decreasing electron density of the PSS brush [7]. Since the choice of slabs is somewhat arbitrary, the brush thickness H is calculated from the first moment: $H = 2 \frac{\int_0^\infty z[\rho(z) - \rho_{\text{sub}}] dz}{\int_0^\infty [\rho(z) - \rho_{\text{sub}}] dz}$. $z = 0$ it set at the PSS adsorption layer/brush interface.

Results.—Diffraction peaks measured along the isotherm are shown in Fig. 1, here on 1 mM CsCl. On monolayer compression, a shift to larger Q_{xy} -values occurs, indicating a decrease of lattice distances. The lateral order has to be ascribed to a strongly structured fluid, not to a crystal; since the lateral correlation length ξ is slightly less than twice the lattice constant [$\xi = 1.6\pi/\text{FWHM}(Q_{xy}^{\text{max}})$, Bragg-peaks are fitted by Gauss-functions]. Equilibrium separation is achieved slowly (compression speed of 0.1 Å²/s or less is necessary). To make sure that equilibrium regarding height and position of the Bragg peak is achieved, and to avoid beam damage (for the most sensitive films, the intensity of a Bragg peak was halved after the sample surface was irradiated by 3.5×10^{13} photons, a slight shift of the peak position to smaller Q_{xy} indicated polymer decomposition), the monolayer is moved laterally

beneath the beam, and the measurements are repeated several times.

To verify that indeed the separation of polyion chains or chain bundles is measured, the electron-rich Cs⁺ counterions were replaced by electron-poor Na⁺. Similar Bragg peaks, yet with less intensity, are observed. Apparently, the main scattering centers are the polyelectrolyte chains, specifically the benzene rings with the sulfonate groups. If a subphase of 1 mM CsCl is chosen (cf. Fig. 1 left and center), then about 2/3 of the counterions within the polyelectrolyte brush are Cs⁺-ions [7]. The electron-rich counterions within the brush improve the contrast, indicating that Cs⁺ accumulate close to the polyelectrolyte chains.

In Fig. 1 (center), the rod-scans along the isotherm are shown. Always, a peak with a maximum at $Q_z = 0$ is found, indicating a vertical alignment of the brushes. On compression, the peak width increases, indicating that the vertical length of the ordered chains within the brush decreases, even though the brush thickens slightly.

Figure 1 (right) shows a reflectivity measurement of a salted brush with 1M CsCl in the subphase. There is one minimum at large Q_z , which can be attributed to the thin (nonswollen) hydrophobic PEE layer. The strongly stretched polyelectrolyte brush causes the interference pattern at low Q_z . Up to three nonequidistant minima can be distinguished. On compression, all minima shift to the left, indicating thickening of both the hydrophobic and the hydrophilic part. Detailed data analysis shows that the PEE thickness is inversely proportional to the molecular area A_{Mol} ; its electron density is consistent with the mass density of bulk PEE [6]. The PEE layer shows all the properties of a nm-thick melt [15]. This is an advantage, since measuring the thickness of the hydrophobic block provides an additional control of the molecular area. The interfer-

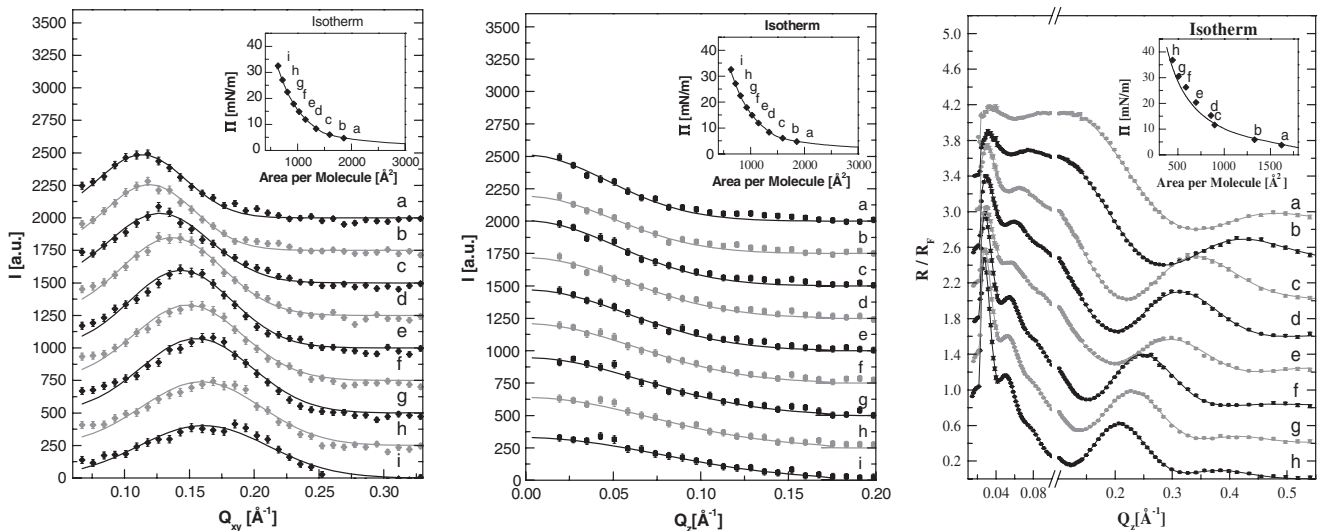


FIG. 1. X-ray studies of PEE₁₄₄PSS₁₃₆ monolayers along the isotherm. The aqueous solution contains 1 mM (left, center) or 1 M CsCl (right). Left: In-plane diffraction peaks with intensity integrated for $0 < Q_z < 0.1 \text{ \AA}^{-1}$. Center: Rod-scans of the data shown left (normalized with respect to the resolution convoluted Yoneda peak) integrated for $0.07 \text{ \AA}^{-1} < Q_{xy} < 0.22 \text{ \AA}^{-1}$. Right: Resolution corrected x-ray reflectivity. The data are shifted vertically relative to each other, the lines are fits.

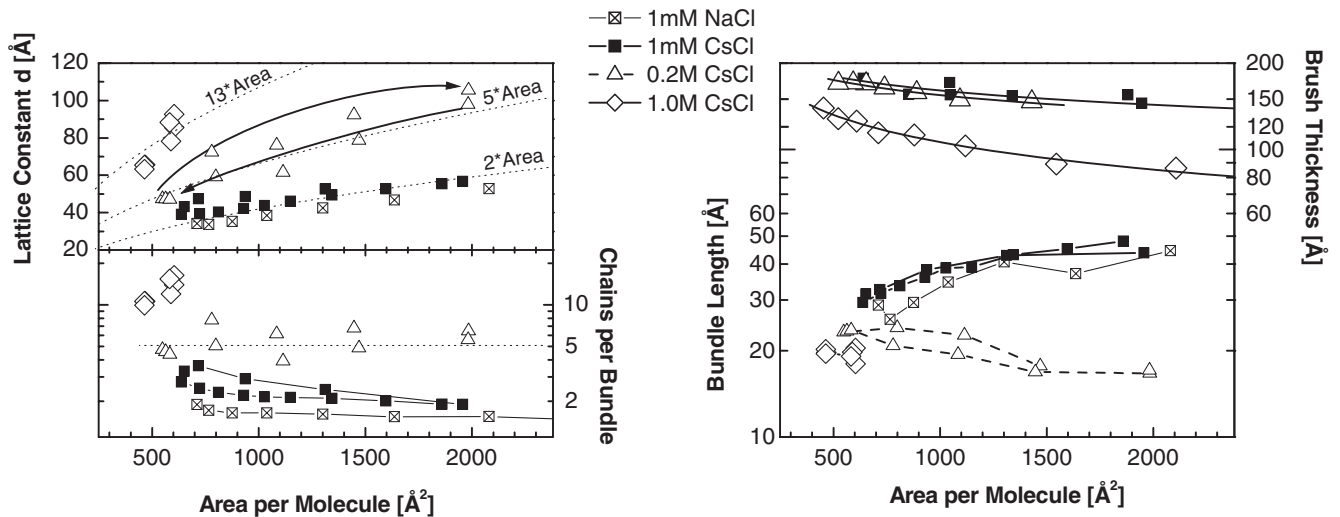


FIG. 2. Results from in-plane measurements in the osmotically swollen phase (full symbols, on 1 mM NaCl and CsCl solution, respectively) and the salted brush phase (open symbols, on 0.2M and 1M CsCl). Left: the measured lattice constant (top) and the deduced chains per bundle (bottom) vs the area per molecule. Compression-Expansion cycles are shown, the larger apparent areas occurring on expansion. The dotted lines indicate the relationship between the area per unit cell and the area per molecule. Right: The bundle length deduced from the rod scans is smaller than the brush thickness obtained from reflectivity measurements.

ence pattern at low Q_z shows an improved contrast on compression, indicating removal of water from the brush, while the Cs incorporation remains constant, and, in the case of the salted brush phase, stoichiometric. The brush thickness is proportional to $A_{\text{Mol}}^{-1/3}$, as theoretically predicted and described for various diblock copolymers with PSS as polyelectrolyte [6,10]. Very clear (due to the improved contrast) and often reproduced is the observation of a flatly adsorbed PSS monolayer of 12 Å thickness directly beneath the hydrophobic block, indicating an attractive interaction between the PSS backbones and the hydrophobic PEE.

Discussion.—The unit cell area A_{cell} deduced from the distance measurements exceeds the molecular area A_{Mol} as determined from the isotherm and the PEE thickness, even assuming a close-packed two-dimensional lattice, i.e., a hexagonal structure with $A_{\text{cell}} = (2/\sqrt{3})d^2$. With increasing salt concentration, the deviation between A_{cell} and A_{Mol} gets more pronounced, from a factor of 2 (osmotically swollen brush with Na^+ counterions) to a factor of about 15 (salted brush with 1M CsCl subphase), cf. Fig. 2. Apparently, not the separation of single chains is measured but the distance between bundles consisting of at least 2 and up to 15 chains, depending on salt conditions. Since the relationship between A_{Mol} and A_{cell} is fairly linear, the aggregation number for a given salt concentration appears to be constant or (at low salt concentration) slightly increases on compression; also, there is a compression/expansion hysteresis.

Spontaneous bundle formation in the bulk phase is theoretically described by molecular dynamic simulations [5,16]. There, divalent counterions are found to be necessary to provide the short-ranged attraction, and the chains

must be sufficiently long and stiff, i.e., the persistence length must be big enough. However, in the experiments described above, no divalent ions provide a short-ranged attraction. Yet, there is evidence of a short-ranged hydrophobic force (which may be seen as a short-ranged attractive solute-solute interaction): PSS is only water-soluble in its charged form, and even then, it adsorbs onto neutral hydrophobic surfaces [6]. The aggregation number is limited by the electrostatic force, which provides a long-ranged repulsion. Its amplitude and range can be decreased by addition of ions into the solution surrounding the polyelectrolytes. Decreased electrostatic repulsion leads to large aggregation numbers in the bundles as we indeed observe (cf. Fig. 2). Qualitatively similar observations have been made for protein solutions and colloidal-polymer mixtures, where a combination of short-range attraction and long-range repulsion results in the formation of equilibrium clusters [17], findings which were supported by model calculations and simulations [18,19].

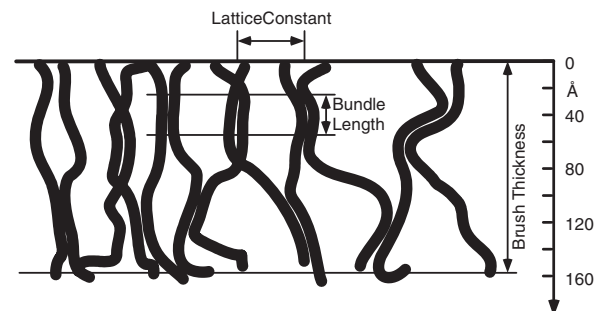


FIG. 3. Scheme of polyelectrolyte brush with spontaneously formed bundles.

We looked for evidence of bundling in micelles of diblock copolymers, yet the many published wide angle scattering studies do not have the necessary resolution. Cryo-transmission electron microscopy provides images. Since the contrast is solely due to counterions, the images represent a map of the counterion distribution. Therefore, micelles (polybutadiene as hydrophobic and polyvinylpyridine as hydrophilic block) with a hydrophobic core appear as light spheres surrounded by a dark corona [20]. Increasing the salt concentration in the solution, thin filaments are observed that extend into the surrounding solution. The filaments have a thickness of about 2 nm, yet a length which is close to the contour length of the polyelectrolyte chains. They probably consist of polyelectrolyte chain bundles containing condensed counterions causing the strong contrast observed in transmission electron microscopy. At 1M salt concentration, filament networks are observed, even for PEE-PSS micelles [20]. While for polyelectrolyte brushes anchored at the air/water interface, a 3-D filament network is impossible, we observe bundling within the brush.

The bundle length as deduced from the rod-scans is smaller than the thickness of the brush. Always, monolayer compression leads to an increase of the counterion concentration within the brush. In the osmotic brush phase, compression causes additionally a slight increase in brush thickness while the bundle length shrinks. At low salt conditions, the polymer chains experience electrostatic stiffening due to the chain charges [1,21]. By increasing salt concentration, the chains get more flexible and the persistence length is reduced. For the same reason, in the osmotic brush phase, an increased counterion concentration shortens the bundles (monomer density 0.8 – 2.5 M).

The increase of the ion concentration in the salted brush leads to a decrease in the brush length. Also, the Debye-length is reduced to a few Å, suggesting that simple electrostatics is no longer sufficient, and the respective molecular volumes should be taken into account. While compression leads to pronounced changes in the brush thickness (theoretically predicted and experimentally found is a change proportional to $A_{\text{Mol}}^{-1/3}$), the bundle length is much smaller and constant, about 20 Å. The constant bundle length is attributed to a constant persistence length of the polyelectrolyte in high salt conditions, since electrostatic stiffening does not occur. Also, salt dependent changes in the conformational fluctuations may be important [22].

Conclusion.—The stretched polyelectrolytes within polyelectrolyte brushes are ideally suited for the study of bundle formation. With x-ray reflectivity and grazing-incidence diffraction, PSS bundles are characterized as function of grafting density and monovalent salt concentration in the subphase. In the osmotic brush phase, bundles consisting of two chains are observed. In the salted brush phase with its large salt concentration, the aggregation

number increases with the salt concentration, up to 15. At the lowest counterion concentrations accessible in an expanded osmotic brush, the bundle length is 50 Å. If the grafting density and thus the counterion concentration are increased, the bundle shrinks. In the high salt concentrations typical for a salted brush, the bundle length is constant as found for the persistence length of a neutral chain. We suggest that the bundle diameter is determined by a balance between long-ranged electrostatic repulsion and short-ranged attraction.

The financial support of the DFG (He 1616 7-4, SFB TR 24) and the BMBF (FKZ 03Z2CK1 with the ZIK HIKE project) is appreciated. Discussions with Burkhard Dünweg and Tanja Schilling were illuminating. We thank HASYLAB at DESY, Hamburg, for beam time and for providing all necessary facilities.

-
- [1] S. Förster and M. Schmidt, in *Physical Properties of Polymers* (Springer Verlag, Berlin, 1995), Vol. 120, p. 51.
 - [2] P.G. de Gennes *et al.*, *J. Phys. (Les Ulis, Fr.)* **37**, 1461 (1976).
 - [3] S. Förster, M. Schmidt, and M. Antonietti, *Polymer* **31**, 781 (1990).
 - [4] V.A. Bloomfield, *Biopolymers* **31**, 1471 (1991).
 - [5] M.J. Stevens, *Phys. Rev. Lett.* **82**, 101 (1999).
 - [6] H. Ahrens, S. Förster, and C. A. Helm, *Phys. Rev. Lett.* **81**, 4172 (1998).
 - [7] H. Ahrens *et al.*, *J. Phys. Chem. B* **108**, 16870 (2004).
 - [8] R. Israels, F.A.M. Leermakers, and G.J. Fleer *et al.*, *Macromolecules* **27**, 3249 (1994).
 - [9] O.V. Borisov, E.B. Zhulina, and T.M. Birshtein, *Macromolecules* **27**, 4795 (1994).
 - [10] J. Rühle *et al.*, *Polyelectrolytes with Defined Molecular Architecture I* (Springer Verlag, Berlin, 2004), Vol. 165, p. 79.
 - [11] K. Kjaer *et al.*, *Phys. Rev. Lett.* **58**, 2224 (1987).
 - [12] J. Als-Nielsen and K. Kjaer, in *Phase Transitions of Soft Condensed Matter*, edited by T.R.a.T. Sherrington (Plenum Press, New York, 1989), Vol. 211, p. 113.
 - [13] V.M. Kaganer, H. Möhwald, and P. Dutta, *Rev. Mod. Phys.* **71**, 779 (1999).
 - [14] H. Ahrens *et al.*, *J. Phys. Chem. B* **108**, 16870 (2004).
 - [15] H. Balthes *et al.*, *Macromolecules* **30**, 6633 (1997).
 - [16] M. Sayar and C. Holm, *Europhys. Lett.* **77**, 16001 (2007).
 - [17] A. Stradner *et al.*, *Nature (London)* **432**, 492 (2004).
 - [18] E. Allahyarov *et al.*, *Europhys. Lett.* **78**, 38002 (2007).
 - [19] W.K. Kegel and P.v.d. Schoot, *Biophys. J.* **86**, 3905 (2004).
 - [20] S. Förster, V. Abetz, and A.H.E. Müller, *Polyelectrolytes with Defined Molecular Architecture II* (Springer Verlag, Berlin, 2004), Vol. 166, p. 173.
 - [21] M. Schönhoff, *J. Phys. Condens. Matter* **15**, R1781 (2003).
 - [22] C. Holm *et al.*, *Polyelectrolytes with Defined Molecular Architecture II* (Springer Verlag, Berlin, 2004), Vol. 166, p. 167.